$\mathbb{Z}_2$ Gauge Field Coupled to a Fermion System

Jinyuan Wu

October 20, 2021

In the whole article we use σ and s as shorthands of σ^z and s^z, unless confusion may be caused by the notation.

1 The model Hamiltonian

The model investigated in this article is shown in [5]. The model Hamiltonian is

$$H = H_Z \underbrace{-J\sum_{\langle \boldsymbol{i},\boldsymbol{j}\rangle}\sigma_{\boldsymbol{ij}}s_{\boldsymbol{i}}s_{\boldsymbol{j}} + \sum_i h_i^x s_i^x}_{H_{\text{Ising}}} - t\sum_{\langle \boldsymbol{i},\boldsymbol{j}\rangle}\sigma_{\boldsymbol{ij}}c_{\boldsymbol{i}}^\dagger c_{\boldsymbol{j}}, \tag{1}$$

where

$$H_Z = -g\sum_{\boldsymbol{l}\in\square_{\boldsymbol{i}^*}}\sigma_{\boldsymbol{ij}}^z - h\sum_{\langle \boldsymbol{i},\boldsymbol{j}\rangle}\sigma_{\boldsymbol{ij}}^x, \tag{2}$$

where $\boldsymbol{i}^*$ is a site in the dual lattice (i.e. a site placed at the center of a plaquette), $\square_{\boldsymbol{i}^*}$ is the plaquette whose center is $\boldsymbol{i}^*$, and $\boldsymbol{l}$ denotes a certain bond of a plaquette. Such kind of model Hamiltonian usually emerges from orthogonal metals [5, 6].

The author of [5] claims that

- The model (1) shows "deconfined *thermal* phase transitions with $\mathbb{Z}_2$ structures".
- The mechanism for a thermal phase transition in a $\mathbb{Z}_2$ theory is that deconfined fermions coupled to the $\mathbb{Z}_2$ gauge field introduces effective interaction between $\mathbb{Z}_2$ charges.
-

We think the author's argument is flawed; yet the model is still interesting and is worth some investigation.

In this section, we introduce every part of (1).

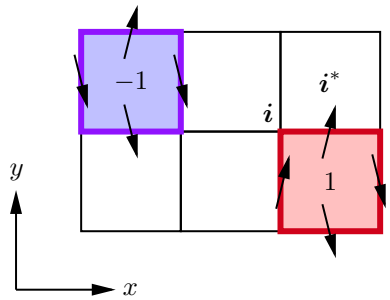

Figure 1: A $\mathbb{Z}_2$ gauge field configuration. The blue plaquette's $F_{\boldsymbol{i}^*}$ is $(-1)\times 1\times(-1)\times(-1) = -1$, while the red plaquette's $F_{\boldsymbol{i}^*}$ is $1\times 1\times(-1)\times(-1) = 1$. Note that we assign the same index to a plaquette's center (labeled as $\boldsymbol{i}^*$ at the right top of the diagram) and the plaquette's left bottom site $\boldsymbol{i}$. The terms "up" and "down" are defined in the Cartesian coordinates given in the diagram.

1.1 $\mathbb{Z}_2$ gauge field and its dual theories

1.1.1 The plaquette term

The plaquette term in the Hamiltonian of the $\mathbb{Z}_2$ gauge field is be a function of

$$F_{i^*} = \prod_{l \in \square_{i^*}} \sigma_l, \tag{3}$$

which is invariant under a $\mathbb{Z}_2$ gauge transformation

$$Q_{\boldsymbol{i}} = \prod_{\boldsymbol{l} \in +_{\boldsymbol{i}}} \sigma^x_{\boldsymbol{l}}. \tag{4}$$

A convenient convention is to let a plaquette share the same index with the site in its left bottom corner. An example of a $\mathbb{Z}_2$ gauge field configuration can be found in Figure 1 on page 1.

1.1.2 The transverse field

We name the $\mathbb{Z}_2$ gauge theory with plaquette terms only as the **Wegner model**, i.e.

$$H_{\mathrm{W}} = -g \sum_{\boldsymbol{i}} F_{\boldsymbol{i}^*}. \tag{5}$$

There is no quantum fluctuation in H_{W}. The existence of interaction between the $\mathbb{Z}_2$ field and the Ising field and the fermions introduces effective interaction channels between $\mathbb{Z}_2$ excitations, but all effective interaction between $\mathbb{Z}_2$ excitations are in terms of $\sigma^z_{\boldsymbol{ij}}$, which commutes with H_Z and therefore do not bring in quantum fluctuation.

An idiomatic way to add quantum fluctuation is to add a transverse field. In this project we consider a transverse field Hamiltonian in the form of

$$H_h = -h \sum_{\langle \boldsymbol{i},\boldsymbol{j} \rangle} \sigma^x_{\boldsymbol{ij}}, \tag{6}$$

where the parameter h measures the quantum fluctuation. (6) obviously commutes with $\boldsymbol{Q_i}$ for every $\boldsymbol{i}$, so it can be a term in a $\mathbb{Z}_2$ gauge invariant Hamiltonian. In the language of string-net condensation, H_h is a string tension term. So when we say "$\mathbb{Z}_2$ gauge theory", usually we are referring to

$$H = -J \sum_{\boldsymbol{i}} \prod_{\boldsymbol{l} \in \square_{\boldsymbol{i}^*}} \sigma_{\boldsymbol{l}} - h \sum_{\langle \boldsymbol{i},\boldsymbol{j} \rangle} \sigma^x_{\boldsymbol{ij}}. \tag{7}$$

1.1.3 Equivalence between a $\mathbb{Z}_2$ gauge theory when $h = 0$ and a bundle of Ising chains

Now we consider a $\mathbb{Z}_2$ field theory with the plaquette term only, or in other words, we investigate the Wegner model. With the gauge choice

$$\sigma_{\boldsymbol{i},\boldsymbol{i}+\hat{\boldsymbol{x}}} = 1, \tag{8}$$

we have

$$F_{i^*} = \sigma_{i,i+\hat{y}} \sigma_{i+\hat{x},i+\hat{x}+\hat{y}}, \tag{9}$$

which, by renaming $\sigma_{i,i+\hat{y}}$ into S_i, reads

$$F_{i^*} = S_i S_{i+\hat{x}}. \tag{10}$$

The hopping constant $\sigma_{\boldsymbol{ij}}$, respectively, is

$$\sigma_{\boldsymbol{ij}} = \begin{cases} 1, & j = i + \hat{x}, \\ S_i, & j = i + \hat{y}, \end{cases}, \quad \sigma_{\boldsymbol{ji}} = \sigma_{\boldsymbol{ij}}. \tag{11}$$

This, actually, means that the $\mathbb{Z}_2$ gauge field may also be transformed into a dual transverse field Ising field. For example consider Wegner model. With the definition of S_is it is rephrased into

$$H_{\mathrm{W}} = -g \sum_i S_i S_{i+\hat{x}}, \tag{12}$$

so the model is actually a bundle of 1D Ising spin chain.

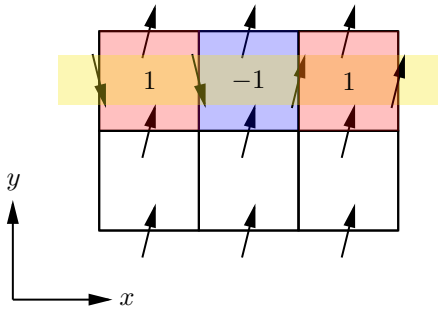

Figure 2: Converting a $\mathbb{Z}_2$ gauge field theory into a bundle of Ising chains. There is no interaction between parallel Ising chains.

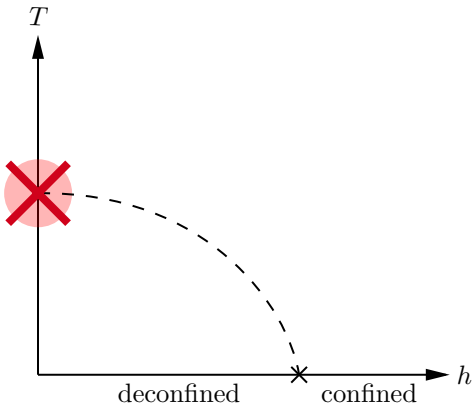

Figure 3: No deconfined phase when $T > 0$: if there is a deconfined phase when $T > 0$, there must be a thermal phase transition at the $h = 0$ line, which is forbidden by the fact that a classical 1D Ising chain does not show thermal phase transitions.

1.1.4 Mapping a $\mathbb{Z}_2$ gauge theory into a 2D transverse field Ising model

$$H = -h \sum_{\langle \boldsymbol{I}, \boldsymbol{J} \rangle} \tau^z_{\boldsymbol{I}} \tau^z_{\boldsymbol{J}} - J \sum_{\boldsymbol{I}} \tau^x_{\boldsymbol{I}}. \tag{13}$$

(13) is often called the **dual transverse field Ising model** of $\mathbb{Z}_2$ gauge theory (7). The model (7), therefore, is often called the **Ising gauge theory**.

1.1.5 Absence of a finite temperature deconfined phase

When $T = 0$ and $h \ll g$, the $\mathbb{Z}_2$ gauge field exhibits a *deconfined* phase, i.e. there are freely moving $\mathbb{Z}_2$ excitations such as $\mathbb{Z}_2$ fluxes.

When $h = 0$, the absence of quantum fluctuation here means the model is indeed totally classical, so there is no thermal phase transition, because a 1D Ising chain does not show thermal phase transition. On the other hand, we know when $T = 0$ the model exhibits deconfined $\mathbb{Z}_2$ charges, and when a transverse field is introduced a zero temperature quantum phase transition can be observed from the deconfined phase into the confined phase as the transverse field grows. If for $T > 0$ there exists a deconfined phase, a simple analysis of the phase diagram tells us there must be a thermal phase transition when there is no transverse field. The fact that Wegner model is dual to a bundle of 1D Ising chain and therefore lacks thermal phase transition implies that no deconfined phase exists with finite non zero temperature.

Here the terminology may cause confusion: we do not actually know if the "finite temperature deconfined" phase shares behavior with the standard zero temperature deconfined phase in Wegner model, and the "confined" phase in the high temperature condition is not caused by a strong transverse field which coerces all σ degrees of freedom into $\rightarrow$ or $\leftarrow$, but rather, by thermal fluctuation that erases all information of $\mathbb{Z}_2$ excitations. With the criteria of Wilson loops we know the "deconfined" phase obeys the perimeter law, agreeing with the ordinary deconfined phase in Wegner model, but whether the Wilson loop operator is a good detector

in non-local models is still under question, because in local models, existence of long range correlation indicates exotic phenomena, while in non-local models long range correlation may be a trivial consequence of the non-locality. All these questions remain open, and in this project we simply use the terms "confined" and "deconfined" as a shorthand of the two phases in a $\mathbb{Z}_2$ gauge field theory with a dual theory of Dyson-Ising spin chains, without inquiring into their similarity and discrepancy with local $\mathbb{Z}_2$ theories such as Wegner model.

1.1.6 (Trivial) deconfined phase in models with long-range interaction

If we are to extend the deconfined phase to $T > 0$, at least some stronger correlation must be introduced. Without introducing quantum fluctuation, a reasonable proposal may be

$$H_Z = -\sum_i \sum_{r=1}^{\infty} J(r) \prod_{a=0}^{r-1} F_{i^*+a\hat{x}},$$

or in terms of S_is,

$$H_Z = -\sum_{r=1}^{\infty} J(r) \sum_i S_i S_{i+r\hat{x}},$$

which is again a bundle of spin chains without quantum fluctuation but this time with long range interaction. A famous example is the **Dyson-Ising chain**, which is defined as

$$H_Z = -g\sum_i S_i S_{i+\hat{x}} - J_r \sum_{\boldsymbol{i}} \sum_r \frac{S_i S_{i+r\hat{x}}}{r^\omega}.$$

For 1D Ising chain with long-range interaction, there exists a thermal phase transition with zero transverse field, and indeed we get a deconfined phase with finite temperature, and as the temperature goes up the deconfined phase switches to the confined phase.

However, the so-called deconfined phase of a long-range interacting model is not of particular interest, because if you put manually something long-range into a model, *of course* it exhibits some long-range behaviors, for example Wilson loops obeying the perimeter law. That is why we call such a "deconfined phase" a trivial one. Despite its triviality, "deconfined" phases in long-range models give us a hint that strong interaction between $\mathbb{Z}_2$ fluxes is important for a thermal deconfined phase. A natural question to ask is, if we introduce more things into the model to induce effective interaction channels between $\mathbb{Z}_2$ fluxes, what happens when $T > 0$?

1.2 Orthogonal metals, emergent fermions and an Ising field

1.2.1 Fermion fractionalization in orthogonal metals and the effective model

Orthogonal metal is a type of fractionalized electron systems where an electron is split into another fermion and an Ising spin, i.e.

$$c^\dagger_{\boldsymbol{i}\alpha} = f^\dagger_{\boldsymbol{i}\alpha}\sigma^z_{\boldsymbol{i}}, \tag{14}$$

where f operators and σ^z operators commute and $f^\dagger_{\boldsymbol{i}\alpha}$ fermions can move around freely. Since the Hilbert space spanned by the f fermions and Ising spins are larger than the original electronic system's Hilbert space, certain constraints must be imposed, resulting in an emergent gauge field, gluing up f and σ fields.

That justifies the way we construct (1). Suppose we have a tight-binding electron models with certain interaction channels that are strong enough to create a non-Fermi liquid phase, the Hamiltonian of which is

$$H = -t\sum_{\langle \boldsymbol{i},\boldsymbol{j}\rangle,\alpha} c^\dagger_{\boldsymbol{i}\alpha} c_{\boldsymbol{j}\alpha} + \sum_{\boldsymbol{i},\boldsymbol{j}} V_{\boldsymbol{ij}} n_{\boldsymbol{i}} n_{\boldsymbol{j}}. \tag{15}$$

Substituting (14) into (15) and doing necessary mean field approximations, we find that the Hamiltonian about f fermions in the model is also a tight-binding Hamiltonian with its hopping constants being the same as $\sigma_{\boldsymbol{ij}}$, which couples the fermions with the $\mathbb{Z}_2$ gauge field, endowing the fermions $\mathbb{Z}_2$ charges.

The idea of orthogonal metals gives us an approach to find a local $\mathbb{Z}_2$ gauge model that shows deconfined phase at finite temperature. Our logic is the inverse of the derivation of orthogonal

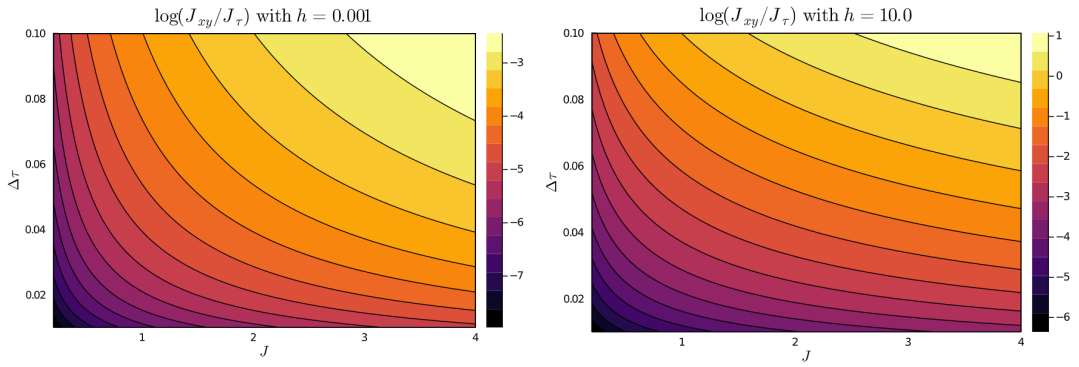

(a) $h = 0.001$ (b) $h = 10$

Figure 4: J_{xy}/J_τ under different h. It can be seen that (17) is highly anisotropic for a large range of J.

metals: if an orthogonal metal with $\mathbb{Z}_2$ gauge structure does exist, then it can be described by (1). That implies the existence of a model Hamiltonian in the form of (1) with a deconfined phase. Our goal is, therefore, to check under what condition (1) *can never* be in a deconfined phase.

1.2.2 Confined phase in orthogonal metals

When the $\mathbb{Z}_2$ charges get trapped into a confined phase, it can be expected that the fermions and the Ising spins are also confined. Note that what the composite particles generated by the gauge field as a glue in the confined phase are is not quite clear. One possibility is that the fermions are glued together, forming something like Cooper pairs, where the fermion excitations are now gapped. Nonetheless, note that orthogonal metals are generated in a strongly correlated *electron* systems, so it is highly likely that *one fermion and one Ising spin* are glued together, restoring the electrons. In this case, the confined phase is just an ordinary metal, with gapless fermions (electrons). At high temperature $\mathbb{Z}_2$ excitations are confined (in the sense defined in Section 1.1.5), so (1) is just an ordinary metal.

2 Principles of Monte Carlo simulation for degrees of freedom in (1)

We are going to study (1) numerically. In the partition function, the (non-normalized) weight of a configuration is $\langle n|\mathrm{e}^{-\beta H}|n\rangle$, given that $\{|n\rangle\}$ is a basis.

In this section we discuss how degrees of freedom in the model can be simulated in quantum Monte Carlo methods. We can use discrete path integral methods or maybe SSE to evaluate these weights.

2.1 The 2D transverse field Ising model

2.1.1 From 2D transverse field Ising model to 3D classical Ising model: discrete path integral and Metropolis update

In this section we use σ to denote spin-1/2 degrees of freedom in a 2D transverse field Ising model. This notation conflicts with the symbol σ for $\mathbb{Z}_2$ gauge field, and is inconsistent with the symbol s for the Ising field, but since we do not deal with the complete (1) it does not matter. We also let $\sigma^z = \{\sigma^z_{\boldsymbol{i}}(\tau)\}$ be the field configuration at τ.

The transverse field Ising model is

$$H_{\mathrm{TFIM}} = -J\sum_{\langle \boldsymbol{i},\boldsymbol{j}\rangle}\sigma^z_{\boldsymbol{i}}\sigma^z_{\boldsymbol{j}} + h\sum_{\boldsymbol{i}}\sigma^x_{\boldsymbol{i}}. \tag{16}$$

We know that a two dimensional quantum statistical model corresponds to a three dimensional classical statistical model, which is because a quantum statistical model can have quantum

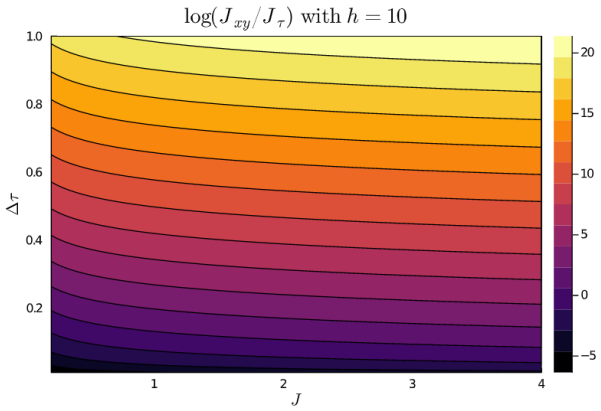

Figure 5: $\log(J_{xy}/J_\tau)$ with extremely large $\Delta\tau$

fluctuation and therefore imaginary time evolution, adding one imaginary time dimension. It is, therefore, a wise idea to write down the discrete path integral formulation of (16), and use the Metropolis algorithm to simulate the discrete path integral, which is a 2+1 dimensional model.

An imaginary time step in the path integral of (16) is

$$\begin{aligned}
\langle\sigma^z(\tau+\Delta\tau)|\mathrm{e}^{-\Delta\tau H}|\sigma^z(\tau)\rangle &= \langle\sigma^z(\tau+\Delta\tau)|\mathrm{e}^{-\Delta\tau\sum_i h\sigma_i^x}\mathrm{e}^{\Delta\tau\sum_{\langle i,j\rangle}J\sigma_i^z\sigma_j^z}|\sigma^z(\tau)\rangle \\
&= \mathrm{e}^{\Delta\tau\sum_{\langle i,j\rangle}J\sigma_i^z\sigma_j^z}\langle\sigma^z(\tau+\Delta\tau)|\mathrm{e}^{-\Delta\tau\sum_i h\sigma_i^x}|\sigma^z(\tau)\rangle \\
&= \mathrm{e}^{\Delta\tau\sum_{\langle i,j\rangle}J\sigma_i^z\sigma_j^z}\sum_{\{\sigma_i^x\}}\mathrm{e}^{-\Delta\tau\sum_i h\sigma_i^x}\langle\sigma^z(\tau+\Delta\tau)|\sigma^x\rangle\langle\sigma^x|\sigma^z(\tau)\rangle \\
&= \mathrm{e}^{\Delta\tau\sum_{\langle i,j\rangle}J\sigma_i^z\sigma_j^z}\prod_{\boldsymbol{i}}\sum_{\sigma_{\boldsymbol{i}}^x}\mathrm{e}^{-\Delta\tau h\sigma_{\boldsymbol{i}}^x}\langle\sigma_{\boldsymbol{i}}^z(\tau+\Delta\tau)|\sigma_{\boldsymbol{i}}^x\rangle\langle\sigma_{\boldsymbol{i}}^x|\sigma_{\boldsymbol{i}}^z(\tau)\rangle \\
&= \mathrm{e}^{\Delta\tau\sum_{\langle i,j\rangle}J\sigma_i^z\sigma_j^z}\prod_{\boldsymbol{i}}\sum_{\sigma_{\boldsymbol{i}}^x=\pm1}\mathrm{e}^{-\Delta\tau h\sigma_{\boldsymbol{i}}^x}\frac{1}{2}\mathrm{e}^{\mathrm{i}\pi\frac{1-\sigma_{\boldsymbol{i}}^x}{2}\left(\frac{1-\sigma_{\boldsymbol{i}}^z(\tau)}{2}+\frac{1-\sigma_{\boldsymbol{i}}^z(\tau+\Delta\tau)}{2}\right)} \\
&= \frac{1}{2^N}\mathrm{e}^{\Delta\tau\sum_{\langle i,j\rangle}J\sigma_i^z\sigma_j^z}\prod_{\boldsymbol{i}}\left(\mathrm{e}^{-\Delta\tau h}+\mathrm{e}^{\Delta\tau h}\mathrm{e}^{\mathrm{i}\pi\frac{1-\sigma_{\boldsymbol{i}}^z(\tau)}{2}}\mathrm{e}^{\mathrm{i}\pi\frac{1-\sigma_{\boldsymbol{i}}^z(\tau+\Delta\tau)}{2}}\right) \\
&= \frac{1}{2^N}\mathrm{e}^{\Delta\tau\sum_{\langle i,j\rangle}J\sigma_i^z\sigma_j^z}\prod_{\boldsymbol{i}}\left(\mathrm{e}^{-\Delta\tau h}+\mathrm{e}^{\Delta\tau h}\sigma_{\boldsymbol{i}}^z(\tau)\sigma_{\boldsymbol{i}}^z(\tau+\Delta\tau)\right).
\end{aligned}$$

The first equation introduces a Trotter error with magnitude $\mathcal{O}(\Delta\tau^2)$. Since $\sigma_{\boldsymbol{i}}^z=\pm1$, we have

$$\cosh J_\tau+\sinh J_\tau\sigma_{\boldsymbol{i}}^z(\tau)\sigma_{\boldsymbol{i}}^z(\tau+\Delta\tau)=\mathrm{e}^{J_\tau\sigma_{\boldsymbol{i}}^z(\tau)\sigma_{\boldsymbol{i}}^z(\tau+\Delta\tau)},$$

so

$$\mathrm{e}^{-\Delta\tau h}+\mathrm{e}^{\Delta\tau h}\sigma_{\boldsymbol{i}}^z(\tau)\sigma_{\boldsymbol{i}}^z(\tau+\Delta\tau)\propto\mathrm{e}^{J_\tau\sigma_{\boldsymbol{i}}^z(\tau)\sigma_{\boldsymbol{i}}^z(\tau+\Delta\tau)},$$

where

$$\tanh J_\tau=\mathrm{e}^{2\Delta\tau h}.$$

So the discrete path integral of (16) with time step $\Delta\tau$ shares its weights with the partition function of the classical Ising model

$$H=-J_{xy}\sum_{\tau,\text{ spacial }\langle\boldsymbol{i},\boldsymbol{j}\rangle}\sigma_{\boldsymbol{i}\tau}\sigma_{\boldsymbol{j}\tau}-J_\tau\sum_{\tau,\boldsymbol{i}}\sigma_{\boldsymbol{i}\tau}\sigma_{\boldsymbol{i},\tau+\Delta\tau} \tag{17}$$

at $T=1$, where

$$J_{xy}=\Delta\tau J,\quad \tanh J_\tau=\mathrm{e}^{2\Delta\tau h}. \tag{18}$$

To ensure high accuracy, we have to use a $\Delta\tau$ small enough, especially for a large h. From Figure 4 on page 5 we can see that when $\Delta\tau$ is large, the contours are more horizontal, or in other words, the change of J may not be reflected faithfully to the change of J_{xy}/J_τ. Since the discrete

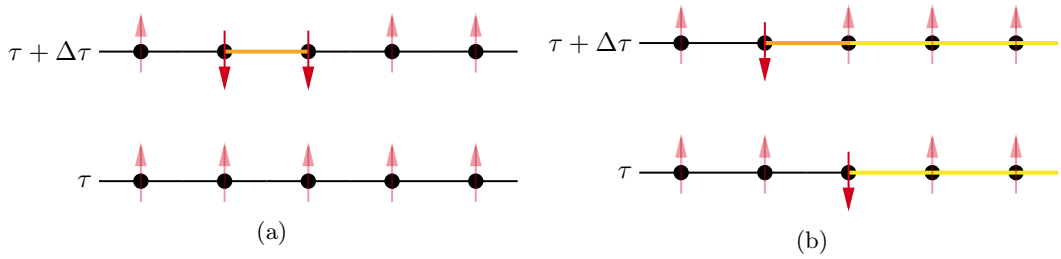

Figure 6: String fragments provided in (22). (a) corresponds to the $\sigma^+\sigma^+$ term, where a minimal string is created out of nothing, or in other words, two magnons are created out of nothing. (b) corresponds to the $\sigma^+\sigma^-$ term, which extends an existing string, or in other words, a magnon is moved to its nearest neighbor. The time inverse of (a) and (b) can be easily found, which are annihilation of a minimal string and shortening an existing string, correspondingly.

path integral will be studied as a classical Ising model (17) under a fixed temperature, the system is characterized by J_{xy}/J_τ, and if J_{xy}/J_τ does not reflect the properties of the transverse field Ising model faithfully the Monte Carlo simulation of (17) does not make any sense. An extreme case can be found in Figure 5 on page 6, where the contours are almost completely horizontal.

Another fact that can be read from Figure 4 on page 5 is that for large h/K $\Delta\tau$ should be smaller to keep the same accuracy. The larger h is, the stronger the quantum fluctuation is, and with strong quantum fluctuation $\Delta\tau$ must be small enough to accurately track the time evolution.

It should be noted, however, that (17) is usually highly anisotropic between time and space, so when $\Delta\tau$ goes too small, the model is hard to simulate with Metropolis algorithm.

2.1.2 Cluster update algorithm along the temporal direction

The anisotropic feature of (17) is tackled in [1].

We did a benchmark of our algorithm with data provided in [3].

2.1.3 Worm algorithm for 2D transverse field Ising model

Another way to simulate 2D transverse field Ising model is described in [4]. We do the following (canonical) substitution

$$\sigma_{\boldsymbol{i}}^x \longrightarrow -\sigma_{\boldsymbol{i}}^z, \quad \sigma_{\boldsymbol{i}}^z \longrightarrow -\sigma_{\boldsymbol{i}}^x, \quad \sigma_{\boldsymbol{i}}^y \longrightarrow -\sigma_{\boldsymbol{i}}^y \tag{19}$$

in (16), and obtain

$$H = -J \sum_{\langle \boldsymbol{i},\boldsymbol{j} \rangle} \sigma_{\boldsymbol{i}}^x \sigma_{\boldsymbol{j}}^x - h \sum_{\boldsymbol{i}} \sigma_{\boldsymbol{i}}^z. \tag{20}$$

which can be viewed as a string-net model, where the $\sum \sigma^z$ term is string tension term and the other term is the string kinetic term. The ends of a σ^z string are two sites on which $\sigma^z = -1$, as opposed to the "vacuum" case where $\sigma^z = 1$. We define the ladder operators in the standard way

$$\sigma_{\boldsymbol{i}}^{\pm} = \frac{\sigma_{\boldsymbol{i}}^x \pm \mathrm{i}\sigma_{\boldsymbol{i}}^y}{2}, \tag{21}$$

then (20) turns into

$$H = -J \sum_{\langle \boldsymbol{i},\boldsymbol{j} \rangle} (\sigma_{\boldsymbol{i}}^+ \sigma_{\boldsymbol{j}}^- + \sigma_{\boldsymbol{i}}^+ \sigma_{\boldsymbol{j}}^+ + \text{h.c.}) - h \sum_{\boldsymbol{i}} \sigma_{\boldsymbol{i}}^z, \tag{22}$$

which can also be rewrite into one of hardcore boson model.

The σ^z strings can expand and shrink, and their ends can hop from one site to its neighbors, according to the first four terms in the Hamiltonian, which are factories of string fragments. This is visualize in Figure 6 on page 7. It should be noted that the $\sigma^+\sigma^+$ term only applies to vacuum, or otherwise it just returns zero. Likewise, the $\sigma^+\sigma^-$ term only applies to existing strings, or otherwise it just returns zero. Two or more minimal strings can be created at the

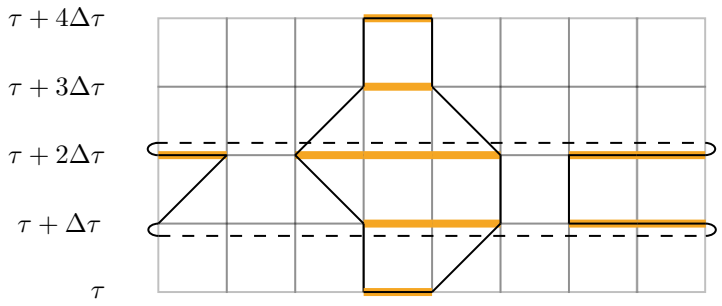

Figure 7: World lines of magnons in a transverse field Ising model model, under the periodic boundary condition. Note that a loop can go across the boundary.

same time, so effectively, a prolonged string can be generated from vacuum in just one time step. As a result, the field configuration used in the path integral is something like this: a string is created, and then distorted, and finally annihilated. So each field configuration used in the path integral is a set of *closed* strings or loops, which are just *world lines* of magnons, as is depicted in Figure 7 on page 8. We name the $\sigma^+\sigma^+ + \text{h.c.}$ terms as **pairing**, the $\sigma^+\sigma^- + \text{h.c.}$ terms **hopping**.

Now we write down the partition function in the path integral form. Suppose there are m time steps. The discrete path integral is

$$Z = \sum_{\{\sigma_\tau\}} \langle\sigma_0|\mathrm{e}^{-\Delta\tau H}|\sigma_\beta\rangle \cdots \langle\sigma_{2\Delta\tau}|\mathrm{e}^{-\Delta\tau H}|\sigma_{\Delta\tau}\rangle \langle\sigma_{\Delta\tau}|\mathrm{e}^{-\Delta\tau H}|\sigma_0\rangle \tag{23}$$

where σ_τ is an arbitrary configuration in the σ^z basis. We classify $\{\sigma_\tau\}$ first according to the number of pairing and hopping, and denote them as N_p and N_h, respectively. The weight of a field configuration with N_p pairing fragments and N_h hopping fragments is

$$\langle\sigma_0|\mathrm{e}^{-\Delta\tau H}|\sigma_\beta\rangle \cdots \langle\sigma_{2\Delta\tau}|\mathrm{e}^{-\Delta\tau H}|\sigma_{\Delta\tau}\rangle \langle\sigma_{\Delta\tau}|\mathrm{e}^{-\Delta\tau H}|\sigma_0\rangle =$$

2.2 The $\mathbb{Z}_2$ gauge theory

2.2.1 Dual transverse Ising model

2.2.2 Simulating $\mathbb{Z}_2$ gauge theory as it is: discrete path integral of $\mathbb{Z}_2$ guage theory

Similar to the case in 2D transverse field Ising model, we may use a discrete path integral to turn the $\mathbb{Z}_2$ gauge theory (7) into a classical statistical model. With the presence of H_h, the H_Z factor of each imaginary time step reads

$$\begin{aligned}
&\langle\sigma(\tau+\Delta\tau)|\mathrm{e}^{-\Delta\tau H_{Z0}}\mathrm{e}^{-\Delta\tau H_h}|\sigma(\tau)\rangle \\
&= \mathrm{e}^{-\Delta\tau H_{Z0}|_{\sigma(\tau)}} \sum_{\sigma^x} \mathrm{e}^{-\Delta\tau H_h|_{\sigma^x}} \langle\sigma^z(\tau+\Delta\tau)|\sigma^x\rangle \langle\sigma^x|\sigma^z(\tau)\rangle \\
&= \mathrm{e}^{-\Delta\tau H_{Z0}|_{\sigma(\tau)}} \sum_{\sigma^x} \mathrm{e}^{h\Delta\tau \sum_{\langle i,j\rangle} \sigma^x_{ij}} \langle\sigma^z(\tau+\Delta\tau)|\sigma^x\rangle \langle\sigma^x|\sigma^z(\tau)\rangle \\
&= \mathrm{e}^{-\Delta\tau H_{Z0}|_{\sigma(\tau)}} \prod_{\text{bond } l} \sum_{\sigma^x_l=\pm1} \mathrm{e}^{h\Delta\tau\sigma^x_l} \langle\sigma^z_l(\tau+\Delta\tau)|\sigma^x_l\rangle \langle\sigma^x_l|\sigma^z_l(\tau)\rangle \\
&= \mathrm{e}^{-\Delta\tau H_{Z0}|_{\sigma(\tau)}} \prod_{\text{bond } l} \sum_{\sigma^x_l=\pm1} \mathrm{e}^{h\Delta\tau\sigma^x_l} \langle\sigma^z_l(\tau+\Delta\tau)|\sigma^x_l\rangle \langle\sigma^x_l|\sigma^z_l(\tau)\rangle\,.
\end{aligned}$$

By the formula

$$\langle\sigma^x_l|\sigma^z_l(\tau)\rangle = \frac{1}{\sqrt{2}}\mathrm{e}^{\mathrm{i}\pi\frac{1-\sigma^x_l}{2}\frac{1-\sigma^z_l(\tau)}{2}},$$

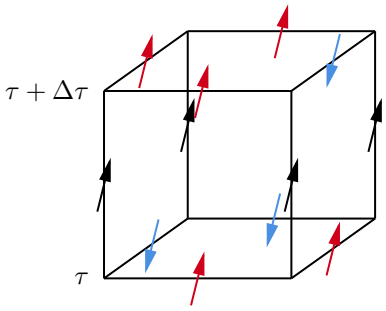

Figure 8: The temporal gauge: the red and blue spin degrees of freedom can rotate arbitrarily, while the black ones (which are on bonds with temporal directions) are fixed to 1.

we have

$$\begin{aligned}
&\langle\sigma(\tau+\Delta\tau)|\mathrm{e}^{-\Delta\tau H_{Z0}}\mathrm{e}^{-\Delta\tau H_h}|\sigma(\tau)\rangle \\
=\ &\mathrm{e}^{-\Delta\tau H_{Z0}|_{\sigma(\tau)}}\prod_{\text{bond } l}\sum_{\sigma_l^x=\pm1}\mathrm{e}^{h\Delta\tau\sigma_l^x}\frac{1}{2}\mathrm{e}^{\mathrm{i}\pi\frac{1-\sigma_l^x}{2}\frac{1-\sigma_l^z(\tau)}{2}}\mathrm{e}^{\mathrm{i}\pi\frac{1-\sigma_l^x}{2}\frac{1-\sigma_l^z(\tau+\Delta\tau)}{2}} \\
=\ &\frac{1}{2^{2N}}\mathrm{e}^{-\Delta\tau H_{Z0}|_{\sigma(\tau)}}\prod_{\text{bond } l}\left(\mathrm{e}^{h\Delta\tau}+\mathrm{e}^{-h\Delta\tau}\mathrm{e}^{\mathrm{i}\pi(\frac{1-\sigma_l^z(\tau)}{2}+\frac{1-\sigma_l^z(\tau+\Delta\tau)}{2})}\right) \\
=\ &\frac{1}{2^{2N}}\mathrm{e}^{-\Delta\tau H_{Z0}|_{\sigma(\tau)}}\prod_{\text{bond } l}\left(\mathrm{e}^{h\Delta\tau}+\mathrm{e}^{-h\Delta\tau}\sigma_l^z(\tau)\sigma_l^z(\tau+\Delta\tau)\right) \\
=\ &\frac{1}{2^{2N}}\mathrm{e}^{-\Delta\tau H_{Z0}|_{\sigma(\tau)}}\prod_{\text{bond } l}\mathrm{e}^{J_\tau\sigma_l^z(\tau)\sigma_l^z(\tau+\Delta\tau)}.
\end{aligned}$$

where

$$\tanh J_\tau = \mathrm{e}^{-2h\Delta\tau}. \tag{24}$$

The last few steps all use the fact that $\sigma_l^z = \pm 1$. So we just need to simulate the "classical $\mathbb{Z}_2$ gauge theory"

$$H = -\Delta\tau J\sum_{\boldsymbol{i},\tau}\prod_{\boldsymbol{l}\in\square_{\boldsymbol{i}^*}}\sigma_{\boldsymbol{l}}(\tau) - J_\tau\sum_{\text{bond }\boldsymbol{l},\tau}\sigma_l^z(\tau)\sigma_l^z(\tau+\Delta\tau) \tag{25}$$

at $T = 1$. (25) actually does not have a $\mathbb{Z}_2$ gauge symmetry, as it can be seen as a 2+1 dimensional $\mathbb{Z}_2$ theory in the path integral formalism with gauge choice

$$\sigma_{\boldsymbol{i},\langle\tau,\tau+\Delta\tau\rangle} = 1, \tag{26}$$

shown in Figure 8 on page 9. This fact actually explains in an intuitively way why (8) does not work: by introducing a transverse field (or string tension term), we have already done an implicit gauge fixing with the form $\sigma = \cdots$, and it is generally impossible to do another like (8).

2.3 Fermion coupling

2.3.1 General ideas of DQMC

Detrimental Quantum Monte Carlo (DQMC) is a discrete path integral for fermions, where an (bosonic) auxiliary field is introduced by Hubbard-Stratonovich transformation and Green functions of the fermions can be recast in terms of the auxiliary field, so we rephrase a fermionic problem into a bosonic one.

The way to simulate fermions coupled to an Ising field with a coupling Hamiltonian in the form of

$$H \propto \sum_{\langle\boldsymbol{i},\boldsymbol{j}\rangle} S_{\boldsymbol{i}}^z S_{\boldsymbol{j}}^z c_{\boldsymbol{i}}^\dagger c_{\boldsymbol{j}} \tag{27}$$

can be found in the appendix of [2].

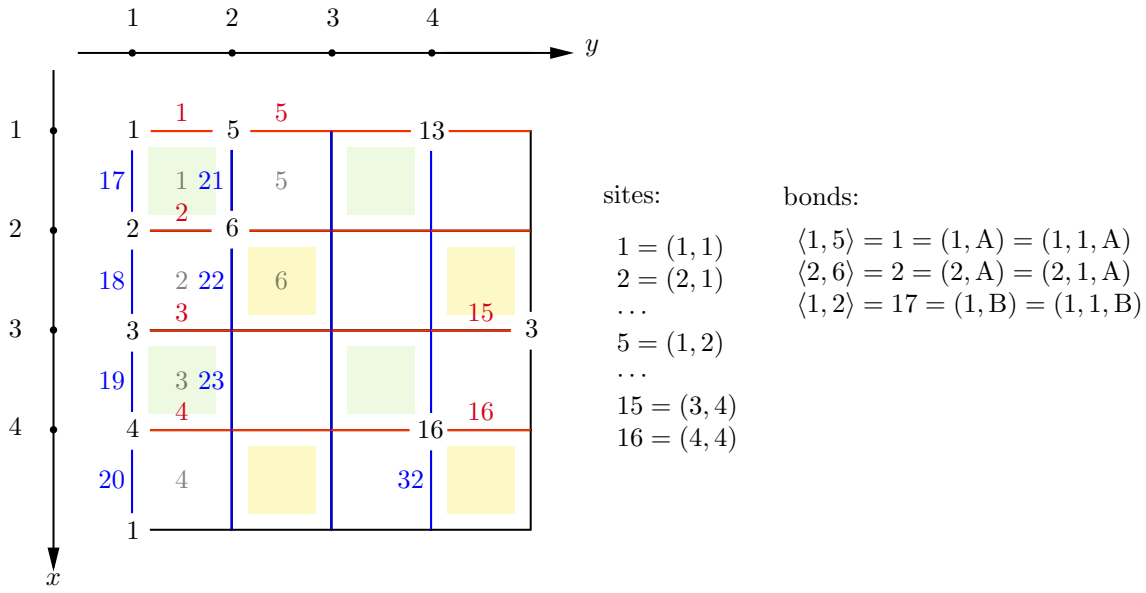

Figure 9: How the lattice is represented in the program. The black numbers placed on sites are the indices of the sites. The red and blue numbers placed on bonds are the indices of the bonds. The bonds form a centered square lattice, and the red numbers correspond to bonds in the A sublattice, the blue numbers the B sublattice. The grey numbers placed on the center of each plaquette is the index of the plaquette.

2.3.2 DQMC for fermion-gauge field coupling in (1)

3 Some details of the program

3.1 The lattice

How the lattice is represented in our program can be found in Figure 9 on page 10. We assign one index to each sites in the 2D periodic lattice. The index agrees with the default column-major order in Julia arrays, if we regard x as the first index and y as the second index of an array, and regard the sites in the lattice as the placeholders of elements in a stringified matrix.

The bonds of the lattice themselves form another lattice, which is a centered square lattice.

The fact that the lattice is periodic is reflected by the fact that, for example, there is a bond between site 4 and site 1, indexed as 20, the coordinate of which in the lattice formed by bonds is $(4, \mathrm{B})$ or $(4, 1, \mathrm{B})$. Note that in the expression $(4, 1, \mathrm{B})$, 1 is the y coordinate instead of the label of site 1.

All plaquettes form a dual lattice, the shape and size of which is exact the same as the lattice shown in the figure. A plaquette shares its index with the top left site, which agrees with Figure 1 on page 1 (note that the two figures' coordinate systems differ in a rotation).

The bonds can be enumerated using a trick called the *check-board decomposition*, where half of the plaquettes are picked out (in Figure 9 on page 10 these plaquettes are painted in green and yellow), the bonds of which are disjoint with each other. For example, plaquette 1 has four bonds, namely bond 1, bond 2, bond 17 and bond 21. These bonds will not be seen in any other bonds colored as green or yellow. On the other hand, if we have N sites, the number of selected plaquettes is $N/2$, and hence the number of bonds attached to the selected plaquettes is $N/2 \times 4$, which is exactly the number of all bonds. The check-board decomposition is useful because it can be noted that if a part of the Hamiltonian is defined as the sum of some operators defined on plaquettes, then operators defined on the green plaquettes commute with each other, and so do the operators defined on yellow plaquettes. An operator defined on the green plaquette does

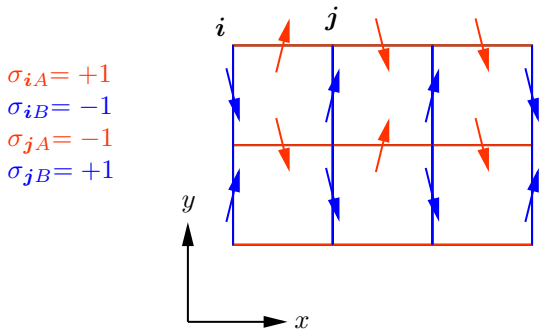

Figure 10: Dividing a gauge field configuration into two sublattices

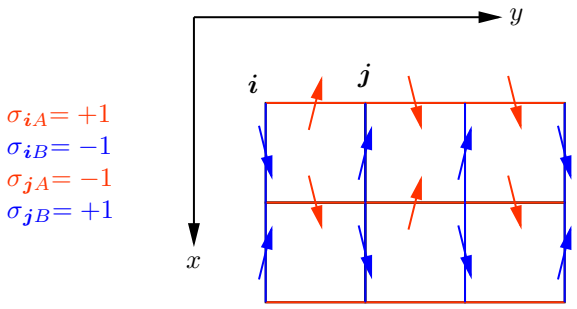

Figure 11: Another way to divide a gauge field configuration into two sublattices, in agreement with Julia's index convention, where `i` in `...[i, j]` means x and `j` means y.

not necessarily commute with an operator defined on the yellow plaquette, so we have

$$\begin{aligned} \mathrm{e}^{-\Delta\tau\sum_{\square_i} O_i} &\approx \mathrm{e}^{-\Delta\tau\sum_{\square_i\in\mathrm{fam}_1} O_i}\mathrm{e}^{-\Delta\tau\tau\sum_{\square_i\in\mathrm{fam}_2} O_i} \\ &= \prod_{\square_i\in\mathrm{fam}_1} \mathrm{e}^{-\Delta\tau O_i} \prod_{\square_i\mathrm{e}^{-\Delta\tau\tau\in\mathrm{fam}_2} O_i} \mathrm{e}^{-\Delta\tau O_i}. \end{aligned} \tag{28}$$

There is still Trotter error, but it only comes from the first step, and as long as $\Delta\tau$ is small enough to make the first equation a reasonable approximation, we can move multiplicative factors in the second equation without introducing additional error. The check-board decomposition, therefore, is a useful method to reduce the Trotter error without having to accept a too small $\Delta\tau$.

3.2 Storage of the $\mathbb{Z}_2$ gauge field

$\mathbb{Z}_2$ gauge degrees of freedom are defined on bonds. Suppose there are N sites. Since there are 4 bonds connecting to one site and a bond is shared by two sites, there are $4N/2 = 2N$ bonds. Therefore, the $\mathbb{Z}_2$ gauge degrees of freedom can be divided into two sublattices, each of which has N degrees of freedom, shown in Figure 10 on page 11. Actually in order to be consistent with Julia's array indexing convention, we choose Figure 11 on page 11 as our convention to label the $\mathbb{Z}_2$ gauge degrees of freedom. Note that the definition of A sublattice and B sublattice in Figure 10 on page 11 is exactly opposite to the definition in Figure 11 on page 11.

4 Simulation of $\mathbb{Z}_2$ gauge theory with different approaches

4.1 Monte Carlo simulation of the pure $\mathbb{Z}_2$ gauge theory with gauge (8)

It should be kept in mind that the gauge (8) is *not* a good gauge choice when a transverse field is introduced. This section, therefore, is mainly about how wrong it is, and whether predictions that are *valid* under (8) - most importantly, no thermal phase transition when $h = 0$ - is observed in the numerical simulation.

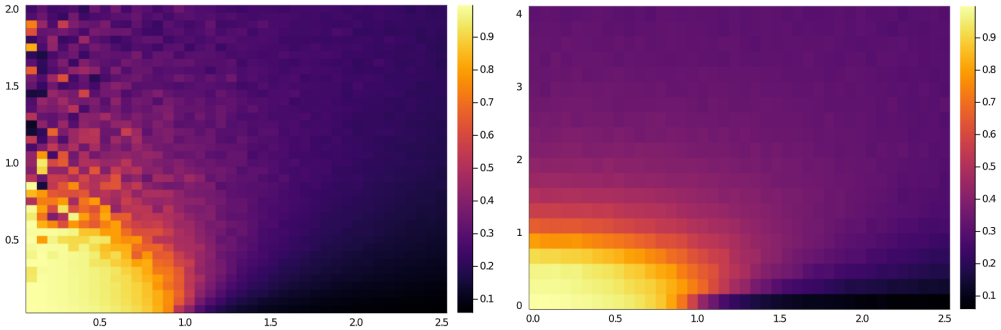

(a) (b)

Figure 12: Magnetization of 1D transverse field Ising chain obtained with different updating algorithms. The x coordinate is h and the y coordinate is T. (a) Metropolis algorithm (b) Wolff cluster algorithm. It can be seen that Metropolis algorithm does not work well when h is small.

4.1.1 The magnetization and the phase diagram

Since J_x and J_y differ a lot, Metropolis algorithm is incapable for the simulation of the anisotropic Ising model. Cluster update methods - in this project Wolff cluster updating [9] - must be used. Figure 12 on page 12 shows a comparison between Metropolis algorithm and Wolff algorithm, where Metropolis algorithm cannot update the system sufficiently when $h = 0$, since in that case the 2D classical Ising modelcorresponding to the 1D transverse field Ising chain degenerates into a classical 1D Ising chain due to the vanishing quantum fluctuation, so the coupling strength in the temporal direction approaches to infinite.

By calculating the magnetic susceptibility we find there is indeed no thermal phase transition. It can be seen in Figure 12 on page 12 that the magnetization changes quite smoothly in the T direction. There is a quantum critical point at $T = 0, h = 1$, which agrees with known theoretical results [7].

Figure 12 on page 12 is therefore qualitatively the same as Figure 3 on page 3. Since (8) is wrong, we will not expect the critical point in Figure 12 on page 12 agrees with the true critical point of the Ising gauge theory on a square lattice.

4.1.2 The area law and the perimeter law

It is kind of surprising - or maybe not that surprising - that under .

4.2 Monte Carlo simulation of the pure $\mathbb{Z}_2$ theory's dual transverse field Ising model

4.2.1 Benchmark of the algorithms

Metropolis and Wolff update for classical Ising model

5 Monte Carlo simulation of the whole model (1)

We introduce a Trotter decomposition with imaginary time step $\Delta\tau = \beta/m$, choose σ_{ij}, s_i as labels for the $\mathbb{Z}_2$ field and the Ising field, respectively, and integrate out the fermion hopping term. Now a configuration of the systems is a sequence of length m, and at each imaginary time

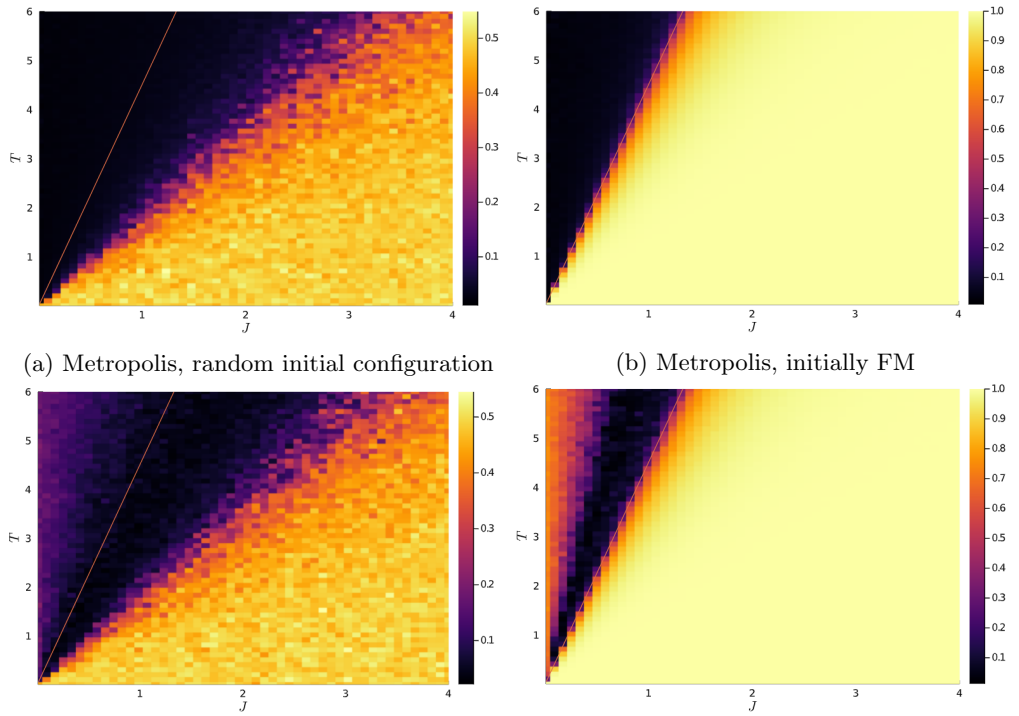

(a) Metropolis, random initial configuration

(b) Metropolis, initially FM

(c) Wolff, random initial configuration

(d) Wolff, initially FM

Figure 13: Simulation of 3D classical Ising modelusing Metropolis update and Wolff update. The data of the straight lines comes from [8].

point τ there is a $\mathbb{Z}_2$ field $\sigma_{\boldsymbol{ij}}(\tau)$ and an Ising field $s_{\boldsymbol{ij}}(\tau)$. The weight of a configuration is

$$\begin{aligned} W(\sigma, s) &= \mathrm{tr}_{\mathrm{fermion}} \prod_{\tau=1}^{m\Delta\tau} \langle(\sigma, s)(\tau + \Delta\tau)|\mathrm{e}^{-\Delta\tau H_Z}\mathrm{e}^{-\Delta\tau H_{\mathrm{Ising}}}|(\sigma, s)(\tau)\rangle\, \mathrm{e}^{\Delta\tau t\sum_{\langle \boldsymbol{i},\boldsymbol{j}\rangle}\sigma_{\boldsymbol{ij}}(\tau)c_i^\dagger c_j} \\ &= \prod_{\tau=1}^{m\Delta\tau} \langle(\sigma, s)(\tau + \Delta\tau)|\mathrm{e}^{-\Delta\tau H_Z}\mathrm{e}^{-\Delta\tau H_{\mathrm{Ising}}}|(\sigma, s)(\tau)\rangle \det\left(1 + \prod_{\tau=1}^{m\Delta\tau} \mathrm{e}^{\Delta\tau t\sigma(\tau)}\right) \\ &= \prod_{\tau=1}^{m\Delta\tau} \langle\sigma(\tau + \Delta\tau)|\mathrm{e}^{-\Delta\tau H_Z}|\sigma(\tau)\rangle\ \langle s(\tau + \Delta\tau)|\mathrm{e}^{-\Delta\tau H_{\mathrm{Ising}}|_{\sigma(\tau)}}|s(\tau)\rangle \det\left(1 + \prod_{\tau=1}^{m\Delta\tau} \mathrm{e}^{\Delta\tau t\sigma(\tau)}\right). \end{aligned}$$

where $\sigma = \{\sigma_{\boldsymbol{ij}}(\tau)\}$ and $s = \{s_{\boldsymbol{i}}(\tau)\}$, and in the last line values of $\sigma(\tau)$ replaces the σ^z operators in H_{Ising}.

References

[1] Henk W. J. Blöte and Youjin Deng. Cluster monte carlo simulation of the transverse ising model. *Physical Review E*, 66(6), December 2002.

[2] Chuang Chen, Tian Yuan, Yang Qi, and Zi Yang Meng. Fermi arcs and pseudogap in a lattice model of a doped orthogonal metal. *Physical Review B*, 103(16), Apr 2021.

[3] Zvi Friedman. Ising model with a transverse field in two dimensions: Phase diagram and critical properties from a real-space renormalization group. *Physical Review B*, 17(3):1429–1432, feb 1978.

[4] Chun-Jiong Huang, Longxiang Liu, Yi Jiang, and Youjin Deng. Worm-algorithm-type simulation of the quantum transverse-field ising model. *Physical Review B*, 102(9), Sep 2020.

[5] Eun-Gook Moon. Deconfined thermal phase transitions with $\mathbb{Z}_2$ gauge structures, 2019.

[6] Rahul Nandkishore, Max A. Metlitski, and T. Senthil. Orthogonal metals: The simplest non-fermi liquids. *Physical Review B*, 86(4), Jul 2012.

[7] Subir Sachdev. *Quantum Phase Transitions*. Cambridge University Press, 2 edition, 2011.

[8] A L Talapov and H W J Blöte. The magnetization of the 3d ising model. *Journal of Physics A: Mathematical and General*, 29(17):5727–5733, Sep 1996.

[9] Ulli Wolff. Collective monte carlo updating for spin systems. *Physical Review Letters*, 62(4):361–364, Jan 1989.